Statistics of volumes, swept by spheroidal particles, in a turbulent flow.

B. Grits*, M. Pinsky, and A. Khain

Institute of Earth Science, The Hebrew University of Jerusalem

1. INTRODUCTION

Collisions between small non-spherical ice crystals determine the formation of larger crystals and snowflakes in clouds. Collisions of non-spherical ice crystals and water drops give rise to the formation of graupel in clouds. As a whole, particle collisions are the key processes determining particles size spectrum evolution. As such they are of crucial importance for understanding and appropriate description of ice microphysics and ice precipitation.

At the same time investigation of these processes is far from being completed due to: a) difficulties in estimation of hydrodynamic forces and torques acting on particles; b) realistic representation of turbulent field, characteristic for cloudy conditions. Due to these difficulties there are only a few theoretical investigations on *droplets* collisions in a turbulent medium at present (e.g. De Almeida, 1976 and 1979; Grover and Pruppacher, 1985; Pinsky *et al*. 1999). All of them indicate that turbulence increases collision rate of cloud droplets several times. It is natural therefore to expect analogous influence of atmospheric turbulence on ice crystals. However no theoretical investigations on ice crystals collisions were reported in literature up to now (Pruppaher and Klett, 1997).

The case of small Stokes number, or Stokesian, particles simplifies significantly the collision problem. In this study we represent a novel approach for evaluation of Stokesian non-spherical particles collision statistics together with preliminary results. Prolate and oblate spheroids were chosen as an example of non-spherical particles. Strongly elongated spheroids can model needle-like ice crystals, while oblate spheroids – plate-like hexagonal prism, one of the most abundant ice crystals form.

---

*Boris Grits, The Department of the Atmospheric Sciences, The Hebrew University of Jerusalem, Givat Ram 91904, Jerusalem, Israel.
Tel: 972 - (2) – 678 – 39 – 07;
Email: bgrits68@yahoo.com

2. STOKESIAN PARTICLES COLLISION

The rate of collisions is determined by collision kernel that describes the probability of collisions between two particles per unit time. It is accepted to represent this probability as the product of collision probability without hydrodynamic interaction (hereafter HDI) between particles and collision efficiency that takes into account the effects of HDI. The rate of collisions with and without HDI is determined by the volume, swept (hereafter referred to as SV) by colliding particles in their relative motion per unit time correspondingly with and without HDI. In this study we limit ourselves by the case *without* HDI.

For turbulent field representation an approach, elaborated by Pinsky *et al.* (2004, 2005), was employed. According to this approach, turbulent field is represented by a set of non-correlated samples of turbulent field. Each sample (hereafter, elementary volume) can be assigned to a certain point of a turbulent flow at a certain time moment. The scales of elementary volume are determined as those within which Lagrangian acceleration of air velocity, $\vec{A}$, and tensor of velocity strains, S, can be considered uniform in space and invariable in time. As was shown by Pinsky *et al.* (2005), these scales are of order Kolmogorov length and time scales. Similar statistical representation of a turbulent flow as a set of small volumes (packets) within which energy dissipation rate, velocity shears and particle concentration were assumed uniform was used recently by Koch and Pope (2002).

Let us introduce the volume, within which HDI is important. Simple scale considerations show that the scales of HDI volume lie within elementary volume for mass equivalent radius $1\mu m \le r_{eq} \le 20\mu m$. This is the particles size range for which one can regard collisions as occurring at constant $\vec{A}$ and S.

To simulate large number of collisions long series (50.000) of S and $\vec{A}$ pairs (field realizations) were produced. These pairs were generated by means of statistical generators, reproducing Largangian accelerations and shears with probability distribution functions (PDFs) found in cloud measurements and laboratory

experiments for high Reynolds numbers (Antonia *et al.*, 1981; Belin *et al.*, 1997; Hill and Thoroddsen, 1997; Kholmyansky *et al.*, 2001; La Porta *et al.*, 2001; Voth *et al.*, 2002).

Another important feature of our approach is that we approximate particle motion in elementary volumes with the help of approximate analytical solution. This solution allows obtaining particle orientation and velocities (translation and angular) probability distribution functions (PDFs). This is a generalization of an approach used by Pinsky *et al.* (2005) for investigation of small cloud *droplets* collisions. The knowledge on these PDFs allows in its turn calculation of SV as the integral over all possible collision variants properly weighted.

Estimation of SV for generated series of $\vec{A}$ and S produce SV series. Mean SV was estimated by averaging over these series. SV PDF was obtained by calculation series histograms.

3. ANALYTICAL SOLUTION

Equations, describing spheroid motion in the creeping flow approximation, are (for, example, Broday *et al.*, 1998):

$$m\frac{d\vec{v}}{dt} = K(\vec{u}-\vec{v}) - mg(1-\frac{\rho_f}{\rho_p})\vec{e_3}\,, \qquad (6)$$

$$I\frac{d\vec{w}}{dt} + \frac{dI}{dt}\vec{w} = Q\left(\Re\times\vec{u}\right) - \Omega\vec{w}. \qquad (7)$$

$\vec{u}$ is a fluid velocity; K, Q and Ω are tensors of particle resistance to translation and rotation. These equations imply: a) small particle Reynolds number approximation; b) assumption on constant S. We apply the method of successive approximations (Korn and Korn, 1968), using solution in the non-inertial limit ($m \to 0$) as a starting point.

3.1 *Translation velocity*

The approximate solution is:

$$\vec{v} = \vec{u} + K_v\left(\vec{e}\right)\cdot\sum_{i=1}^{\infty}\vec{G_i}\left(\vec{e}\right), \qquad (8)$$

Matrix K_v and vectors $\left\{\vec{G_i}\right\}$ are functions of spheroid orientation, $\vec{e}$. Consequently spheroid velocity deviation from air velocity, $\vec{v'} = \vec{v} - \vec{u}$, is also function of its orientation only. This solution provides relatively simple recurrent relation for vectors $\left\{\vec{G_i}\right\}$.

Let's define Stokes number to be $St \equiv \tau_t / \tau_f$. Here $\tau_t \approx 10^{-3}\,s$ characterizes particle adjustment time to fluid translation, and $\tau_f \approx 1/Sh$ is a characteristic time of fluid velocity variation (Sh - characteristic shear). The truncation error is of order $\left(St\right)^k$, k being first neglected term in (8). For example, omitting terms of order $i \geq 2$ for $St = 0.04$ (corresponds to $r_{eq} = 20\mu m$) one obtains truncation error less then 0.2%. The important consequences of (8) are that $\vec{v'}$ is defined basically by the Lagrangian acceleration of the fluid and increases approximately as a^2. Both these conclusions imply $St \ll 1$.

3.2 *Angular velocity*

The approximate solution is:

$$\vec{w} = K_w\left(\vec{e}\right)\cdot\left[\vec{\xi}\left(\vec{e}\right) + \sum_{i=1}^{\infty}\vec{R_i}\left(\vec{e}\right)\right]. \qquad (9)$$

$\vec{\xi}$ is the spheroid angular velocity in the non-inertial limit. Matrix K_w and vectors $\vec{\xi}$ and $\left\{\vec{R_i}\right\}$ are all functions of spheroid orientation. Consequently spheroid angular velocity is also determined by orientation. Again there exists recurrent relation for vectors $\left\{\vec{R_i}\right\}$. The truncation error in (9) scales again as $\left(St\right)^k$.

If exact solutions of (6) and (7) are bounded (stable behavior), then any arbitrary initial velocity approaches quickly (on time scale of τ_t) to a solution, shown schematically in **fig.** 1 by a dashed line (limit solution). Solutions (8) and (9) do not describe transient processes but converge directly to this solution. We therefore refer to them as *limit* solutions. Main inaccuracy when using (8) and (9) arises rather due to the difference between limit and exact solutions than due to truncation procedure. This difference however is small for small St. If exact solutions of (6) and (7) are unbounded (unstable behavior), solutions (8) and (9) diverge. It means that they can not describe the so-called sling effects. Such events however are rare for Stokesian particles in atmosphere (Pinsky *et al.*, 2005).

To check solutions (8) and (9), we compared them with numerical solution of (6) and (7) in several situations: a) simple shear flow; b) Poiseuille flow; c) realization of turbulent filed. In all the cases the difference did not exceed 0.1%.

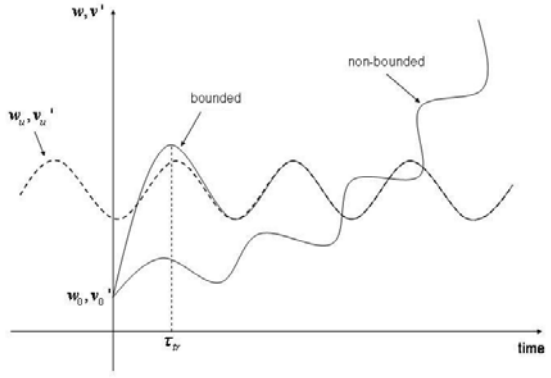

Fig. 1 Stable and unstable velocity scenarios. Limit solution is shown by dashed line.

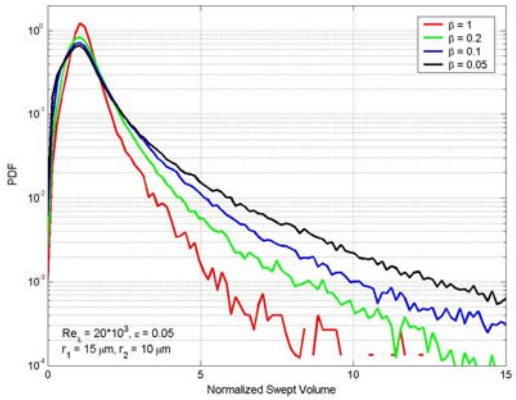

Fig. 2 SV PDFs for oblate spheroids with r_{eq} $15\mu m$ and $10\mu m$

4. RESULTS

We calculated mean SV and SV PDF for a wide range of turbulent field parameters: $5\times10^3 \le \mathrm{Re}_\lambda \le 20\times10^3$ and $0.002 \le \varepsilon \le 0.1$ (Re_λ - Taylor scale based Reynolds number; ε - energy dissipation rate). This range covers cloudy turbulence from stratiform up to deep cumulus clouds. The calculations were performed for spheroids of different sizes ($1\mu m \le r_{eq} \le 20\mu m$) and different aspect ratios ($0.05 \le \beta \le 20$). Here we present some of the results.

Fig. 2 shows SV PDF (histogram) for pair of oblate spheroids with radii $15\mu m$ and $10\mu m$ ($\mathrm{Re}_\lambda = 20\times10^3$, $\varepsilon = 0.05 m^2 s^{-3}$). **Fig**. 3 shows mean SV for the pair of prolate spheroids with equivalent radii $15\mu m$ and $10\mu m$ ($\mathrm{Re}_\lambda = 20\times10^3$). **Fig** 4 shows the same results for oblate spheroids of the same mass. SV is normalized everywhere by SV in a pure gravity case. **Figures** 5 and 6 give analogous results for spheroids with equivalent radii $2\mu m$ and $1\mu m$. **Fig**. 7 and 8 show SV for prolate and oblate spheroids of similar size: $r_{eq1} = 15\mu m$, $r_{eq2} = 15\mu m - \delta r_{eq}$. Reynolds number in this case is 20×10^3, dissipation rate – $0.05\, m^2 s^{-3}$. δr_{eq} varies between $0.2\mu m$ and $1\mu m$. The results manifest that:

- SV PDF differs significantly from Gaussian due to enhanced large SV part of distribution.
- turbulence magnifies mean SV for several tenth of percent comparing with the pure gravity case; the effect enlarges with flow intensity.
- mean SV for spheroids is higher than that for droplets of the same mass; the effect enlarges with aspect ratio deviation from unity, being more pronounced in case of elongated spheroids.
- influence of turbulence on mean SV becomes especially large for small particles (of order $1\mu m$) and particles of similar size.

The proposed method incorporates three main approximations: a) small particle Reynolds number approximation; b) assumption on constant $\vec{A}$ and S during collision; c) approximation of motion equations solution by means of the limit solution. While it is not possible to evaluate error due to the second approximation, one can check the validity of the first and third approximations.

To check small Reynolds approximation we evaluated characteristic value of spheroid Re in all 50.000 realizations and calculated the part, in which Re turned out to be larger than 0.1. While for $r_{eq} = 15\mu m$ spheroid accuracy turned out to be sufficient in all cases, for $r_{eq} = 20\mu m$ error becomes large for intensive turbulent field. For $r_{eq} = 2\mu m$ all realizations resulted in $\mathrm{Re} < 0.1$.

To check the third approximation we compared numerical and limit solutions and calculated the part of realizations, in which this difference exceeded 5%. Again $r_{eq} = 15\mu m$ spheroid provided sufficient accuracy. Accuracy for $r_{eq} = 20\mu m$ spheroid was sufficient in the case of oblate spheroid, but in the case of elongated form and intensive turbulent field it became low. For $r_{eq} = 2\mu m$ spheroid accuracy was again excellent in all cases.

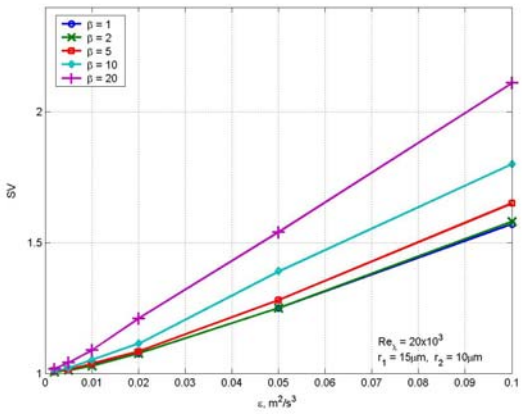

Fig. 3 Mean SV for the pair of prolate spheroids (r_{eq} are $15\mu m$ and $10\mu m$) as a function of dissipation rate.

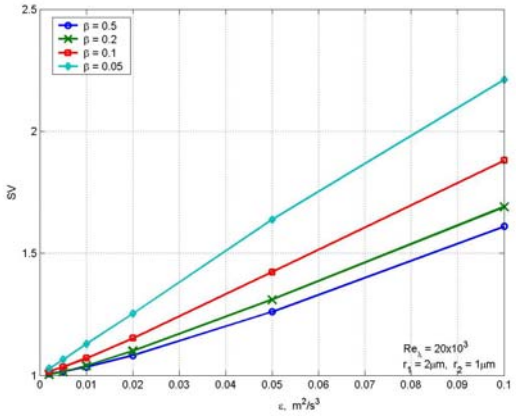

Fig. 6 The same as in fig. 3 for oblate spheroids with r_{eq} $2\mu m$ and $1\mu m$.

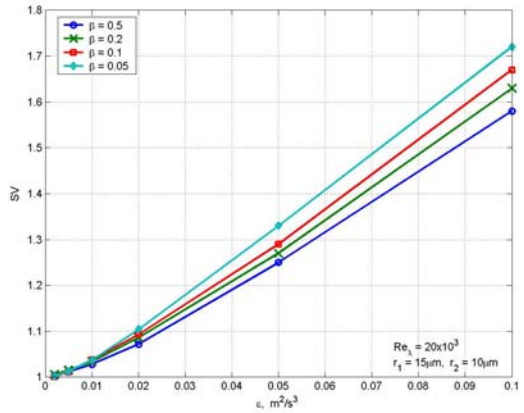

Fig. 4 The same as in fig. 3 for oblate spheroids of the same masses.

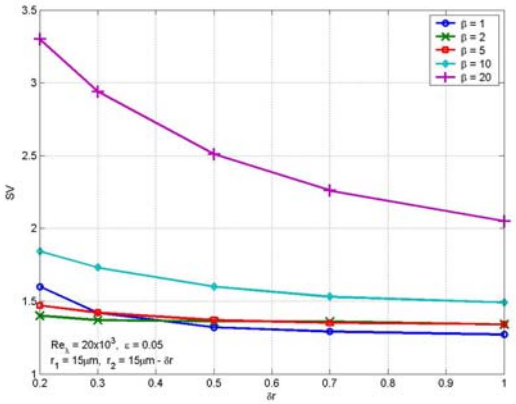

Fig. 7 Mean SV for the pair of prolate spheroids (r_{eq} are $15\mu m$ and $15\mu m - \delta r_{eq}$) as a function of δr_{eq}.

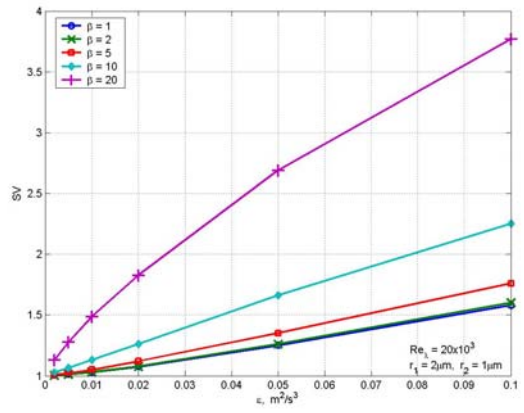

Fig. 5 The same as in fig. 3 for prolate spheroids with r_{eq} $2\mu m$ and $1\mu m$.

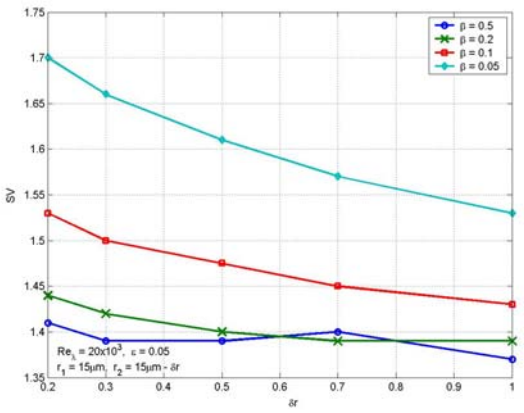

Fig. 8 The same as in fig. 7 for oblate spheroids of the same masses.

As a whole, together with the restriction due to assumption on constant field parameters, $r_{eq} \approx 20\mu m$ may be regarded as the upper limit for the validity of the method proposed. It is worthy noting, however, that the errors due to both small Reynolds and employment of limit solution reduce quickly with decreasing ε and for $\varepsilon = 0.01 m^2 s^{-3}$, for example, main limitation comes from the assumption on constant $\vec{A}$ and *S*.

5. CONCLUSIONS

A novel approach is elaborated for investigation of Stokesian non-spherical particles collisions in a turbulent field, characteristic for cloudy conditions. Turbulent field is represented as a large set of small field samples (elementary volumes), within which field parameters may be regarded constant in space and time. Approximate analytical solution of spheroids motion equations in a general shear flow is found and employed for description of spheroid motion in elementary volumes. This solution allows obtaining spheroid orientation and velocities PDFs. The statistics of SV (PDF and mean value) is estimated by means of averaging over SV series, calculated for generated series of elementary volumes. This approach may be applied for estimation of collision statistics both with and without HDI. In the present, first, stage the case without HDI was regarded.

SV PDF and mean value were calculated for the wide range of turbulent field parameters, representing turbulence intensity from stratiform up to deep cumulus clouds, and for different spheroids sizes and aspect ratios (from strongly elongated up to plate-like forms). The results indicate that turbulence enhances SV significantly comparing with the pure gravity case. The effect increases with turbulence intensity and aspect ratio deviation from unity, and becomes especially pronounced in case of similar and micron size spheroids.

Analysis shows that for spheroids mass equivalent radii $1\mu m \le r_{eq} \le 20\mu m$ the approach proposed may be regarded valid. It is worthy noting however that this range depends on turbulent field intensity and for calm enough turbulence (e.g. $\varepsilon = 0.01 \div 0.02 m^2 s^{-3}$) it may be wider.

ACKNOWLEDGEMENTS

The study was conducted under support of the Israel Academy of Science Foundation grant 173/03) and The Israel Ministry of Science (German-Israel collaboration in Water Resources, grant WT 040).

REFERENCES

Antonia, R.A., Chambers A.J., and Satyaprakash B.R. 1981: "Reynolds number dependence of high order moments of the streamwise turbulent velocity derivative," *Boundary-layer Met*. **21**, 159-171.

Belin F, Maurer J, Tabeling P. and Willaime H., 1997: "Velocity gradient distributions in fully developed turbulence: An experimental study," *Phys. Fluids,* **9**, 3843-3850.

Broday D., Fichman M., Shapiro M. and Gutfinger C., 1998: Motion of spheroidal particles in vertical shear flows. *Phys. Fluids* **10** (1), 86.

De Almeida, F. C., 1976: The collisional problem of cloud droplets moving in a turbulent environment—Part I: A method of solution. *J. Atmos. Sci.,* **33,** 1571–1578.

——, 1979: The collisional problem of cloud droplets moving in a turbulent environment. Part II: Turbulent collision efficiencies. *J. Atmos. Sci.,* **36,** 1564–1576.

Grover, S. N., and H. R. Pruppacher, 1985: The effect of vertical turbulent fluctuations in the atmosphere on the collection of aerosol-particles by cloud drops. *J. Atmos. Sci.,* **42,** 2305–2318.

Hill R. J. and S. T. Thoroddsen, 1997: "Experimental evaluation of acceleration correlations for locally isotropic turbulence," *Phys. Rev.* E, **55**, 1600-1606.

Kholmyansky M., Tsinober A. and Yorich S., 2001: "Velocity derivatives in the atmospheric surface layer at $\mathrm{Re}_\lambda = 10^4$," *Phys. Fluids* **13**, 311-314.

Koch, D.L. and S.B. Pope, 2002: Coagulation-induced particle-concentration fluctuations in homogeneous, isotropic turbulence. *Phys. Fluids*, **14**, n.7, 2447-2455La Porta A., G.A. Voth, A. M. Crawford, J. Alexander and E. Bodenschatz, 2001: "Fluid particle accelerations in fully developed turbulence," *Nature*, **409**, 1017-1019.

Maxey M.R., 1987: The gravitational settling of aerosol particles in homogeneous turbulence and random flow fields. *J. Fluid Mech*. **174**, 441.

Monin, A. S. and A. M. Yaglom, 1975: "*Statistical fluid mechanics: Mechanics of turbulence*," v.2, MIT Press.

.

Pinsky M.B., Khain A.P., and Shapiro M., 1999: Collisions of small drops in a turbulent flow. Pt.1: Collision efficiency: problem formulation and preliminary results. *J. Atmos. Sci.* **56**, 2585.

Pinsky M., Shapiro M., Khain A. and Wirzberger H., 2004: "A statistical model of strains in

homogeneous and isotropic turbulence," *Physica D*, **191**, 297-313

Pinsky M.B.,. Khain A.P., Grits B. and Shapiro M., 2005: Collisions of cloud droplets in a turbulent flow. Part 3. Relative droplet fluxes and swept volumes. *J. Atmos. Sci* (in press).

Pruppacher H.R. and Klett J.D., 1997: Microphysics of clouds and precipitation. Oxford Press.

Voth, G.A., A.La Porta, A. M. Crawford, J. Alexander and E. Bodenschatz, 2002: "Measurements of particle accelerations in fully developed turbulence," *J. Fluid Mech,* **469**, 121-160.